

# Design, Analysis and Fabrication of A Mini-Sailplane for Didactic Purposes In the Area of Development of UAV's/MAV's


 Open  
Access

 Mohd Danish<sup>1</sup>, Zainul Arfin<sup>1</sup>, Azhar Jamil<sup>1,\*</sup>, Syed Mohd. Yahya<sup>1</sup>
<sup>1</sup> Aligarh Muslim University, Aligarh, Uttar Pradesh, 202002, India

## ARTICLE INFO

### Article history:

Received 31 January 2019

Received in revised form 21 February 2019

Accepted 4 March 2019

Available online 22 March 2019

## ABSTRACT

This paper is dedicated towards the design and fabrication of a mini sailplane with the aim of maximizing the glide ratio  $C_L/C_D$ . And at the same time minimizing the weight of the plane. For this NACA 7037 airfoil was selected for subsonic domain corresponding to low Reynolds number varying within the range of  $10^5$  to  $3 \times 10^5$  as per the recommendations from literature [1]. A cambered NACA 7037 was fabricated from the wooden material and was experimentally investigated with different range of velocities and angle of attack for coefficient of lift and drag using wind tunnel setup. The same was numerically investigated using the commercial Finite Element Analysis FEA code of ANSYS FLUENT®. The results compared very well with the experimental one, thereby validating the computational fluid dynamics CFD model. This CFD model was applied to mini sailplane which has cambered profile made up of Balsa wood. Initially, flow around the wing was investigated in order to determine the optimal design for wing by comparing lift, lift-to-drag ratio, stalling characteristics and pitching moment. Finally, the entire sailplane was analysed to get the overall aerodynamic characteristic of the assembly. Main-plane and tail-plane distance was optimized along with the areas of the control surfaces for maximizing L/D ratio and certain designing rules were established. Drag, lift coefficient and pitching moment have been discussed and the appropriate conclusion was drawn. The experiment and calculation showed a significant improvement in the sailplane performance after using an optimized wing configuration.

### Keywords:

 Sailplane Design, Coefficient of Lift,  
 Coefficient of Drag, CFD, ANSYS FLUENT

Copyright © 2019 PENERBIT AKADEMIA BARU - All rights reserved

## 1. Introduction

With the emergence of unmanned air vehicle *UAV* and micro air vehicle *MAV*, the aerodynamic characteristics of airfoil for Reynolds number less than  $5 \times 10^5$  is becoming actively important thereby making the area of high-lift airfoil as a topic of great interest. Most of the existing design procedures are primarily based at higher Reynold number regimes, involving fast and robust analysis of conventional design of airfoil. At Reynolds number less than  $5 \times 10^5$ , the quest becomes a bit severe owing to the transitional separation of boundary layer, bubble formation and transition of laminar to

\* Corresponding author.

E-mail address: [azharjamil@zhcet.ac.in](mailto:azharjamil@zhcet.ac.in) (Azhar Jamil)

turbulent flow related to the Low Reynolds number airfoil [1]. In this work a mini sailplane is designed by maximizing the glide ratio  $C_L/C_D$  corresponding to Low Reynolds number regime. Proper low camber airfoil shape was judiciously selected for a fixed Mach number, Reynolds number and attacking angle as adding camber to the airfoil increases the amount of lift at a fixed angle of attack [2]. The performance characteristics were obtained by numerical simulations with appropriate boundary conditions and were validated experimentally using wind tunnel setup in accordance with the works of D. Greer *et al.*, [3]. At high Reynolds number the boundary layer in airfoil becomes turbulent rapidly and is able to tolerate the adverse pressure gradient with minimum disturbance. The selection of turbulence model for the simulation also plays a vital role in validating the experimental analysis [4].

Sailplanes or gliders were built much before the first human flight was recorded. Chinese were the first to design the true gliders according to the extensive records of the Taiping Era during the 5th century BC. Otto Lilienthal was the first to perform the successful gliding flights in the late 19th century. This design had slow forward speed and sink rate of about 1m/s and provided a descent lift versus drag ratio of about 6 [5]. The revolutionary advancement in the sailplane design came with the prototype testing by the Wright brothers in the early 1900's. This design gave the idea that an aircraft can be controlled by changing the geometry of the sailplane rather than shifting the centre of gravity as done earlier. Development in sailplane design slowed during Second World War but during 1957 the Phoenix was able to achieve the glide ratio of 40:1 due to the introduction of laminar flow airfoils and Eppler airfoil sections especially for sailplane design [6]. There have been many successful approaches that have been applied to aircraft optimization depending upon the optimization strategies and fidelity of the analysis methods. The levels of fidelity analysis have been defined for structural and fluid analysis by Bartholomew [7]. The majority of aircraft design optimization uses low fidelity analysis method as the work by Neufeld *et al.*, [8]. The optimization of sailplane winglets and sailplane wing/fuselage combinations were conducted by Maughmer [9] and Boermans *et al.*, [10]. They further demonstrated the importance of an efficient aerodynamic design for an unpowered aircraft. Flow behaviour of winglet using the Whitcomb winglet was reported by Yahya *et al.*, [11] revealing the reduction of induced drag. The effect of Winglet Cant Angle was examined by Munshi *et al.*, [12] for ONERA M6 transonic wing at different angle of attack and performance of the wing with further optimisation was estimated.

Furthermore, sailplane now-a-days has got a lot more applications than before like underwater glider. Stommel [13] was the first to introduced the concept of underwater glider. Numerical study on the aerodynamic characteristics of both static and flapping wing with attachments are presented by few researchers [14, 15]. Comparative aerodynamic properties of the corrugated dragonfly airfoil, with that of traditional smooth NACA 2.5411 airfoil at low Reynolds number, was reported by Uppu *et al.*, [16]. Jaffar *et al.*, [17] conducted experimental and numerical investigations to study the low speed aerodynamic and stability characteristic of a canard configured aircraft.

## 2. Methodology

The methodology involved in the design of the sailplane involves the selection of airfoil, based on the typical speed of the moving airplane, i.e. the corresponding Reynolds number. This is followed by experimental wind tunnel testing with the acquisition of test data from which numerical procedure involving computational fluid dynamics (CFD) are established. This is utilised in the development of the numerical model using the commercial *FE* code of ANSYS FLUENT<sup>®</sup>. The results so obtained are compared with the experimental data and thereby validation is made. The validated model is then

extended in the study of airflow on the sailplane configuration from which the design is finalised. The whole methodology can be summarised in the form of a schematic diagram as shown in Figure 1.

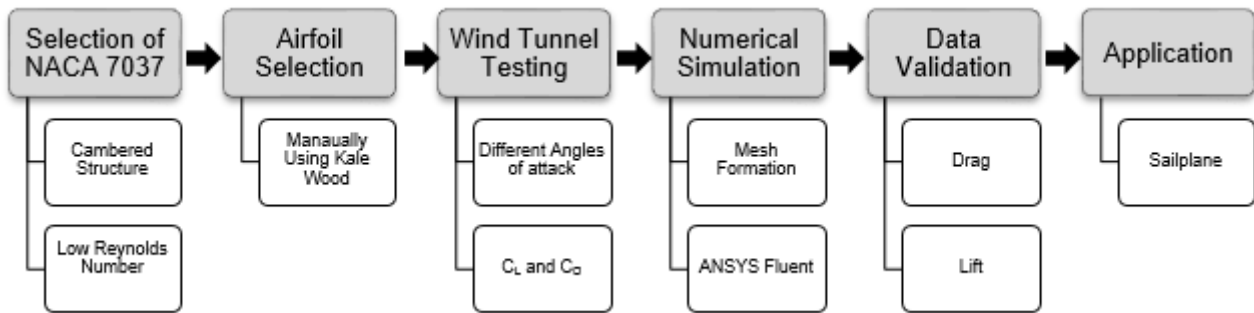


**Fig. 1.** Schematic diagram of the methodology so involved

### 2.1. Airfoil Selection

Airfoil selection plays an important role in the dynamic characteristic for a low Reynolds number sailplane. A curved wing is more efficient than a flat wing. Air moves cleanly over the top, which causes lower pressure to develop with less drag. The air becomes turbulent as it flows over the top leads to inefficient flat wing. Turbulence results in more drag and ultimately, less lift as shown in Figure 2. As per the recommendations by Michael *et al.*, [18] airfoil NACA 7037 has been selected for the sailplane because of its optimum cambered wing design structure to provide better glide ratio. Comparative study of different airfoil configurations, presented by the same author [18] is shown in Figure 3. The airfoil NACA 7037 is most widely used for the fabrication of sailplane as it increases lift on one side and simultaneously decreases drag for better flight. Camber is added to the airfoil in order to increase the lift at comparatively low speeds, however with increase in lift coefficient the stalling speed of sailplane reduces. Aircrafts with cambered wing design usually have lower stalling speed compared with aircrafts with symmetric airfoil section [19]. Javaid *et al.*, showed that the rectangular wing provides larger lift forces but with a reduced stability envelope. Conversely, the tapered wing exhibits lower lift force but improved dynamic stability [20].

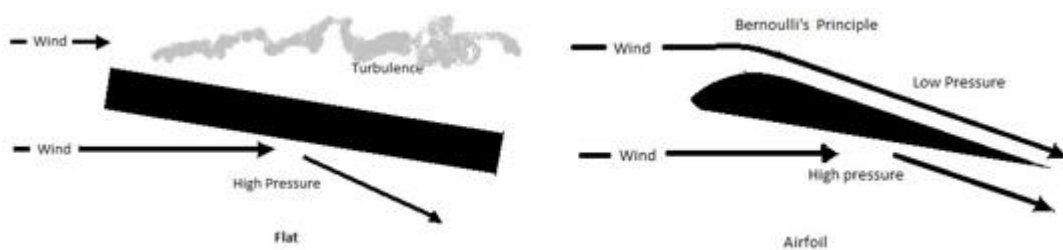


**Fig. 2.** Comparison between flat and cambered airfoil wing configuration

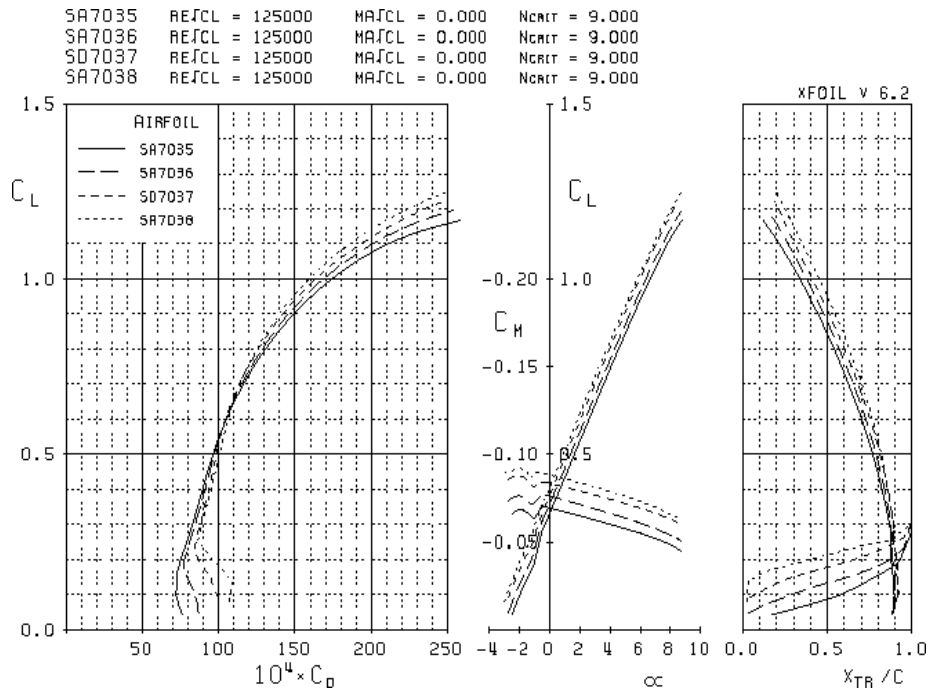


**Fig. 3.** Dependency of different parameters for airfoils SA7036, SD7037 and SA 7038 [18]

Hence for optimal design NACA7037 was selected and with the help of Airfoil Tool® the coordinates of NACA7037 were generated and plotted in Figure 4.



**Fig. 4.** Cambered airfoil section for NACA7037 (t/c = 9.5%)

## 2.2. Fabrication of Airfoil and Wind Tunnel Testing

The fabrication of airfoil was done at the departmental production facility with chord length of 140 mm and span of 300 mm. The airfoil was fabricated at reduced scale as per the limits of the wind tunnel apparatus as seen in Figure 5 (a). The airfoil was tested at the in house subsonic wind tunnel testing facility having a test section of 300 mm wide by 300mm high and 600mm long. The experiment was conducted for 12m/s and 22m/s to get the required results. The measured turbulence intensity in the wind tunnel, as seen in Figure 5(b), was less than 2%. The lift and drag force was measured via force balance method setup having two load transducers calibrated before the start for each test.



(a) AF100 Subsonic Wind Tunnel test setup

(b) NACA 7037 Airfoil made of Kale wood

**Fig. 5.** Wind tunnel setup and airfoil specimen tested at different AoA

### 2.3. Modelling and Simulation

After the experimental quest, modelling of the airfoil was carried upon, with the establishment of numerical model in ANSYS FLUENT®. The airfoil profile was generated in both two and three dimensions using the pre-processor of the software and the flow properties were inputted, represented in Table 1. In order to determine the airflow around the airfoil, the flow domain is divided into mesh which was quadrilateral dominated having four nodes at the corner as shown in Figure 6.

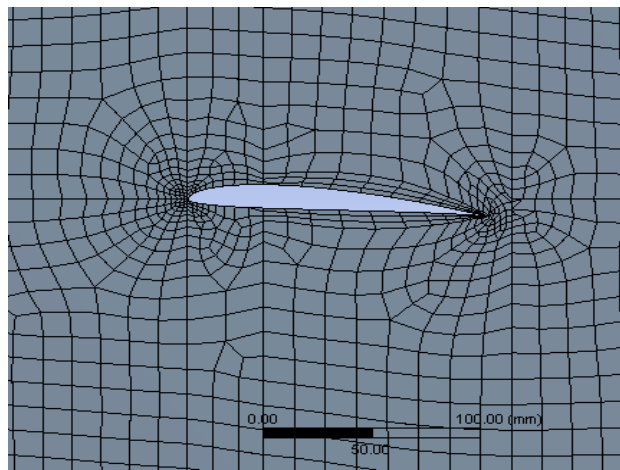


**Fig. 6.** Meshed Region

**Table 1**

Flow properties of air

Air Property	Value	Unit
Density	1.13	kg/m <sup>3</sup>
Kinematic viscosity	1.5668×10 <sup>-5</sup>	m <sup>2</sup> /s
Temperature	299	K

Specific parameters and boundary conditions were applied for specific areas of the mesh. One equation Spalart Allmars (S-A) and pressure based solver was used because of low Reynolds number regime [4] and very low Mach number. Second order functions were applied for more accurate solution. In this work, simulation was performed for Reynolds number varying from 10<sup>5</sup> to 2×10<sup>5</sup> with consequent change in angles of attack from -4<sup>0</sup> to 10<sup>0</sup>. Finally, the aerodynamic forces were

measured for each simulation, in order to determine the coefficient of lift, coefficient of drag and other related parameters.

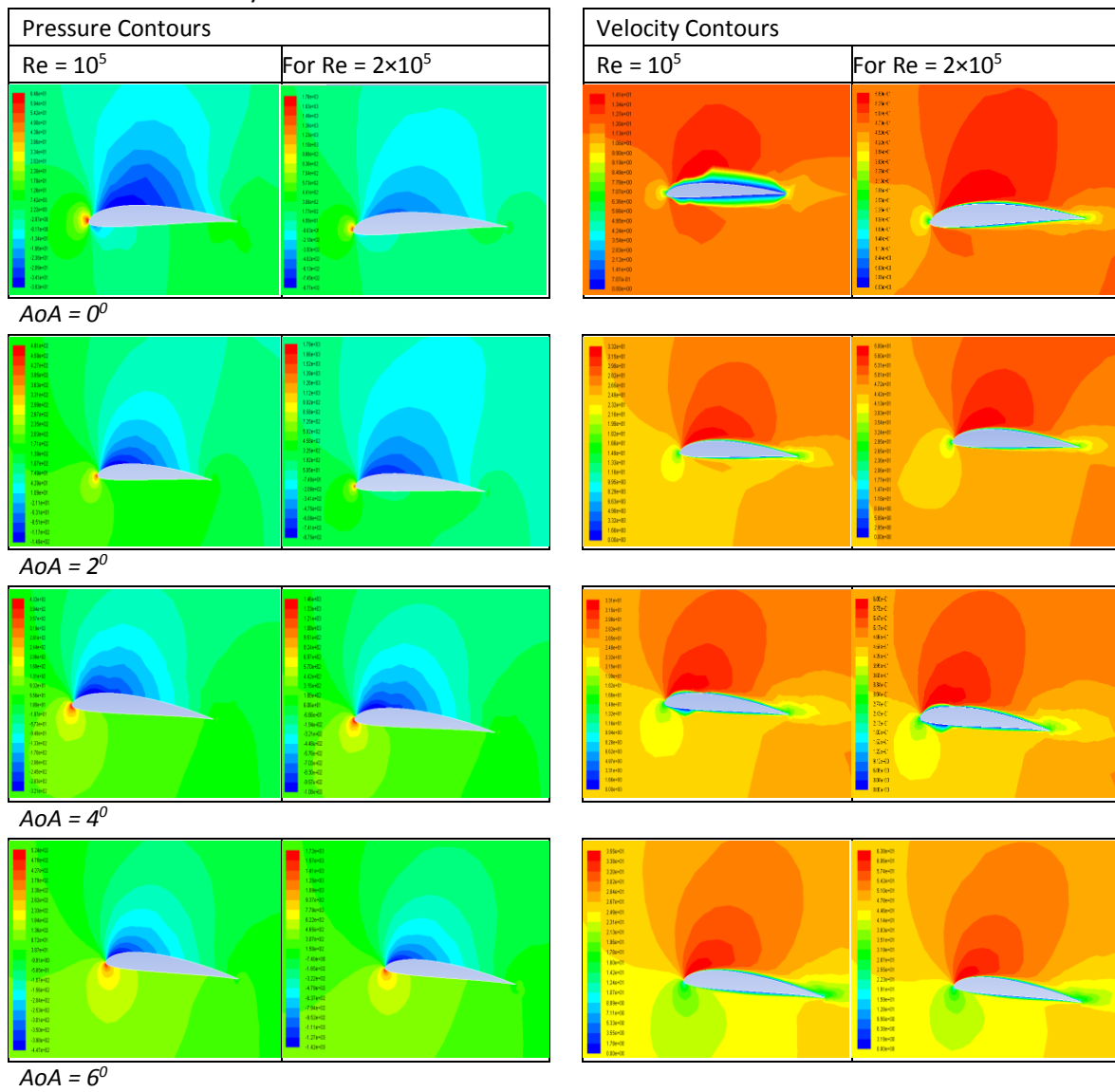
The model so created after validation was further extended for modelling airflow over the full sailplane. The goal is to optimize the glide ratio (lift/drag) by maintaining the proper distance between the main-plane and tail-plane.

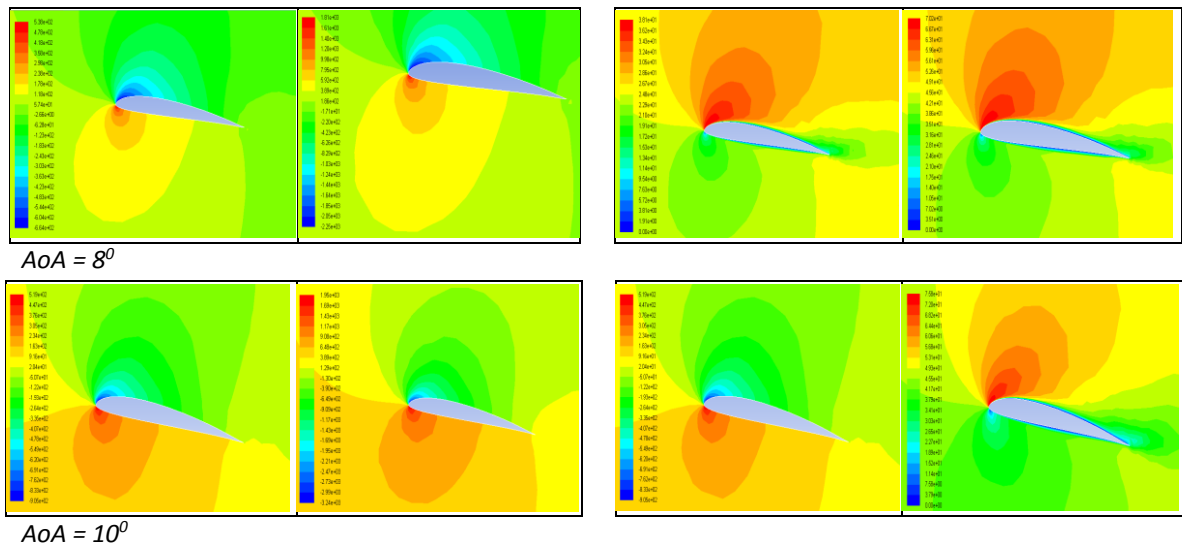
### 3. Results and Discussion

#### 3.1. NACA 7037 Airfoil

The results were obtained by varying the angle of attack from  $-4^{\circ}$  to  $10^{\circ}$  with increment of  $2^{\circ}$ . The velocity and pressure profiles for different Reynold's number against AoA for two different laminar flow regimes are given in the Table 2.

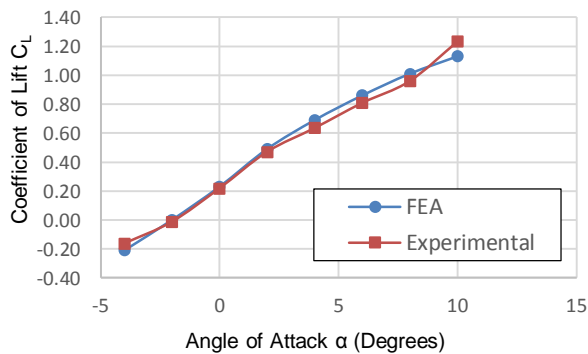
**Table 2**  
 Pressure and velocity Contours for different AoA



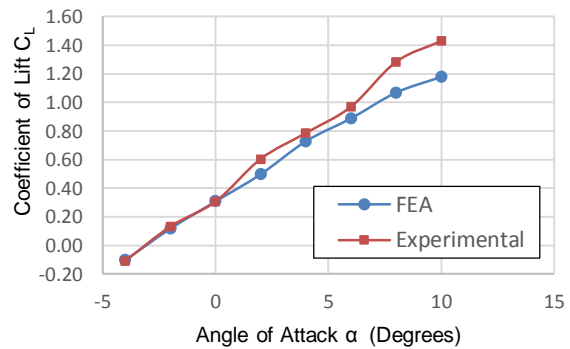


### 3.2. Lift and Drag Characteristics of the Airfoil & Comparison with Wind Tunnel Experimental Data

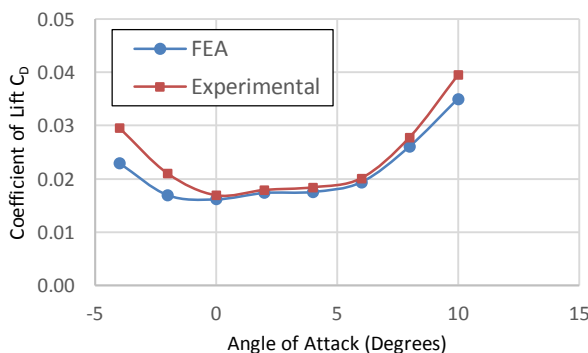
Using force balance, lift was calculated for  $Re = 10^5$  to  $Re = 2 \times 10^5$ . The comparison of numerical lift and drag calculations with the experimental ones was made for different Reynolds number over the entire range of angles of attack are shown in the Figure 7.



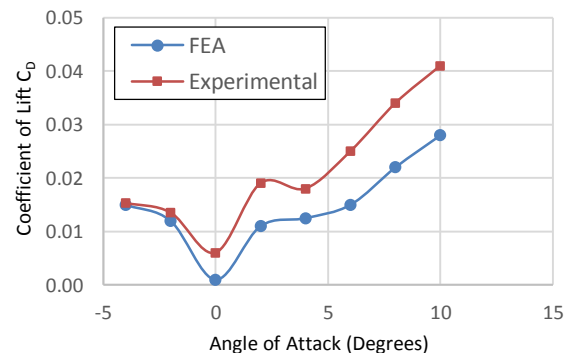
(a)  $C_L$  vs.  $AoA$  for  $Re = 10^5$



(b)  $C_L$  vs.  $AoA$  for  $Re = 2 \times 10^5$



(c)  $C_D$  vs.  $AoA$  for  $Re = 10^5$



(d)  $C_D$  vs.  $AoA$  for  $Re = 2 \times 10^5$

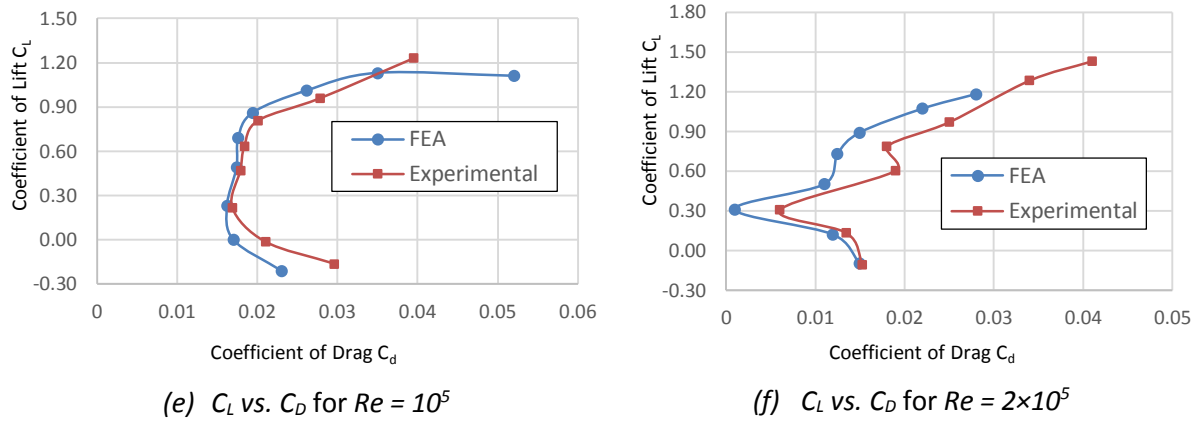


**Fig. 7.** Comparative aerodynamic characteristic plots

The above presented data shows that the manufactured airfoil fairly matches with the NACA 7037 in terms of lift and other related aerodynamic parameters. For higher value of Reynolds number the airfoil develops comparatively more lift and simultaneously produces more drag. Therefore,  $Re = 10^5$  was selected for designing the sailplane and  $Re = 10^5$  gives fairly high lift and low drag depending upon angle of attack provided. From the perspective of lift and operating Reynolds number ( $Re = 10^5$ ) it is plausible to apply these results for the sailplane design. Further, a comparison between glide ratio ( $C_L/C_D$ ) and  $AoA$  was plotted showing the maximum value of glide ratio corresponding to  $6^\circ$  of  $AoA$ , as seen in Figure 8.

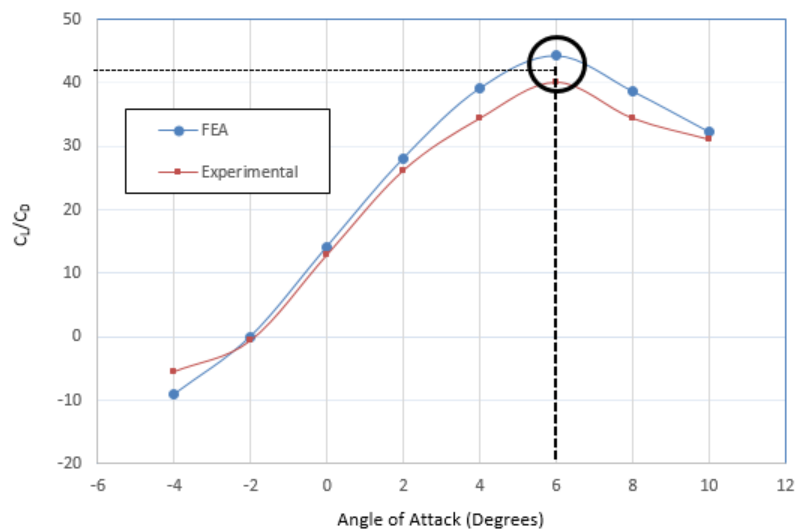


**Fig. 8.**  $C_L/C_D$  vs.  $AoA$  for  $Re = 10^5$

This led to the selection of optimum angle of attack of  $6^\circ$  corresponding to the  $C_L/C_D = 40$  for designing sailplane.

### 3.3. Sailplane Analysis

For  $Re = 10^5$  and  $AoA=6$  degrees the airflow and optimum distance between the mainplane and tailplane assembly were analysed by varying the distance between mainplane and tailplane. The contours for the mainplane and tailplane assembly as seen in Figure 9 revealing the optimum distance of 105mm corresponding to a maximum glide ratio of 33.107, as seen in Table 3.

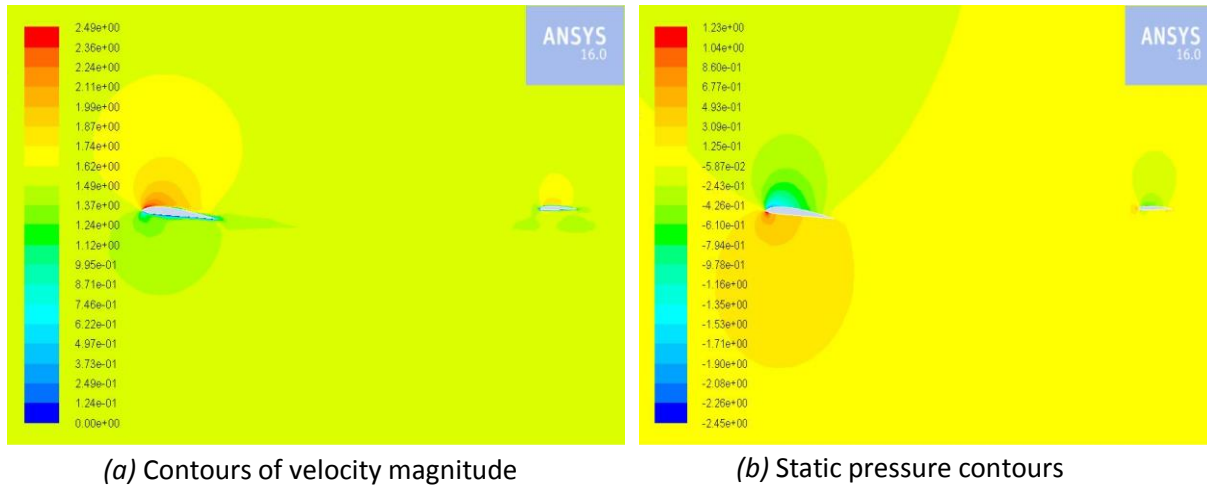


**Fig. 9.** Velocity & Pressure Contours for mainplane & tailplane assembly

**Table 3**  
 Variation of  $C_L$ ,  $C_D$  and  $C_L/C_D$  w.r.t. distance between mainplane and tailplane

Distance (mm)	Coefficient of Lift $C_L$	Coefficient of Drag $C_D$	Glide Ratio $C_L/C_D$
140	1.1654	0.036476	31.94977519
105	1.0894	0.032905	33.10743048
100	1.0937	0.034575	31.63268257
70	1.0828	0.035152	30.80336823

### 3.4. Final Sailplane Design

For the given optimal angle of attack obtained  $6^\circ$  and glide ratio 33.107 and wing-span  $L$ , the length of fuselage was evaluated by with the help the following expression mentioned by Frati [21]

$$M = 0.3L + 2.5 \tag{1}$$

Where,  $M$  is the total length from nose to tail in meters.

For tail plane configuration, angle and location of horizontal tail was determined from criteria shown following the:

- i) Determination of center of gravity  $COG$  position.
- ii) Calculation of attitude of equilibrium without intervention of any control surface (normal flight attitude). This attitude is one corresponding to intersection between  $COG$  line and moment curve.

Having established this attitude of equilibrium, the possible angle of horizontal tail was evaluated and tail span was fixed at 45-60% of fuselage length. From the parameters so obtained, final sailplane was designed with the dimensions in millimetres represented in Figure 10.

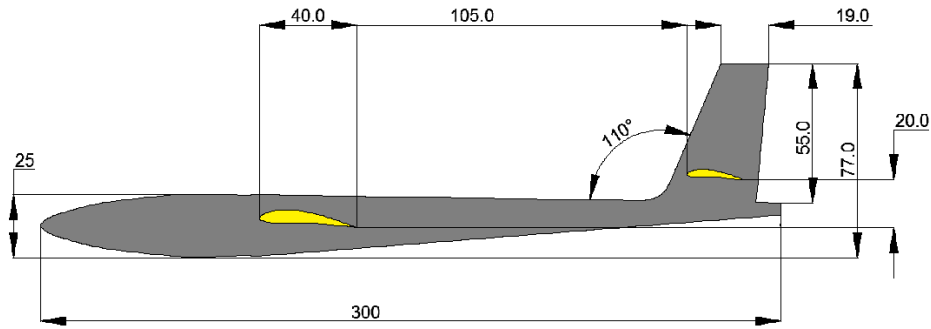
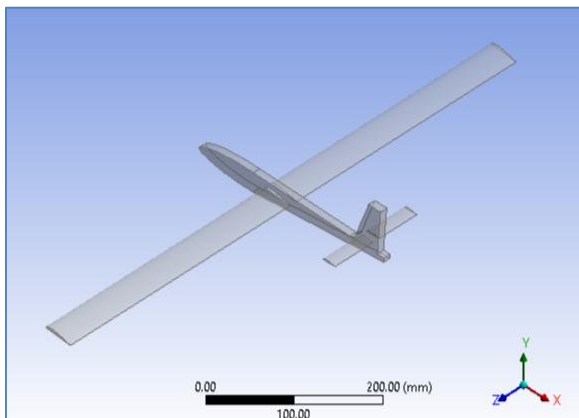


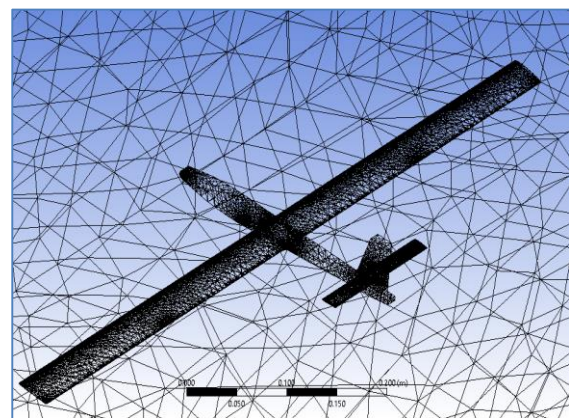
**Fig. 10.** Final dimensions of the Sailplane

A CAD model was finally developed in Solidworks®, as seen in Figure 11(a) and the model was finally simulated on ANSYS FLUENT® revealing the velocity and pressure contours. The mesh grid, velocity and pressure contours are respectively represented in Figures 11(b - d).

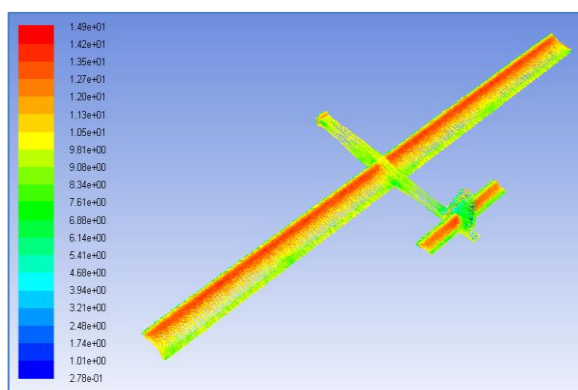
The glider was finally fabricated using Balsa wood, as seen in Figure 11(e). Additional weight in the form of a metal strip were added at the nose in order to bring the centre of gravity at the desired position. The final designed sailplane was finally fabricated, as shown in Figure 11(f).



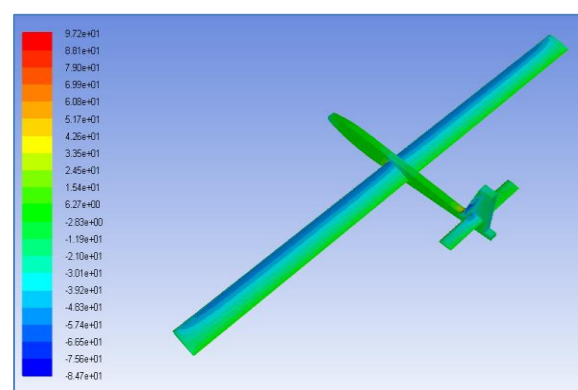
(a) CAD model of the final design



(b) Mesh grid



(c) Velocity Contours



(d) Pressure Contours



(e) Fabrication process



(f) Final fabricated sailplane

**Fig. 11.** CAD model, simulation results, fabrication and the final design of the sailplane

#### 4. Conclusion

From the experimental to the numerical quests made in the design, selection of airfoil and ultimately coming up to the actual sailplane, various conclusions can be drawn.

- Low Reynolds number, in accordance with natural and man-made flyers is verified for low speed of around 10m/s, therefore this regime is proposed for both sailplanes as well as MAV's performance capabilities involving missions such as environmental monitoring, surveillance and assessment in hostile environments.
- Because of low speeds, sailplane poses great challenges towards their aerodynamic stability. Hence in order to design a sailplane for low Reynolds regime requires high level testing and analysis.
- *CFD* results of the numerical simulation matched fairly with the experimental analysis of the airfoil thereby confirming the validity of the approach and in turn the design of the sailplane itself.
- An optimum value of  $AoA$  of  $6^\circ$  was obtained corresponding to maximum glide ratio  $C_L/C_D$  on the basis of which optimum distance between the mainplane and tailplane was evaluated to be equal to 105mm, after the application of the validated *CFD* Model.
- Hence the methodology adopted in this work can be extended in designing low Reynolds number  $Re$  aircrafts, *MAVs* along with sailplanes.

#### References

- [1] Drela, Mark. "XFOIL: An analysis and design system for low Reynolds number airfoils." *In Low Reynolds number aerodynamics*, pp. 1-12. Springer, Berlin, Heidelberg, 1989.
- [2] B. G. B. McCullou and W. M. Haire, "National advisory committee for aeronautics," 1950.
- [3] Greer, Don, Keith Krake, Phil Hamory, Mark Drela, and Seunghee Lee. "A High Altitude-Low Reynolds Number Aerodynamic Flight Experiment." (1999).
- [4] Aftab, S. M. A., AS Mohd Rafie, N. A. Razak, and K. A. Ahmad. "Turbulence model selection for low Reynolds number flows." *PloS one* 11, no. 4 (2016): e0153755.
- [5] Thomas, Fred. "100 YEARS OF SAILPLANE DESIGN AND BEYOND." *Technical Soaring* 27, no. 3-4 (2003): 61-74.
- [6] Maughmer, Mark. "The Evolution of Sailplane Wing Design." *In AIAA International Air and Space Symposium and Exposition: The Next 100 Years*, p. 2777. 2003.
- [7] Markish, Jacob, and Karen Willcox. "Multidisciplinary techniques for commercial aircraft system design." *In 9th AIAA/ISSMO Symposium on Multidisciplinary Analysis and Optimization*, p. 5612. 2002.
- [8] Neufeld, Daniel, Joon Chung, and Kamran Behdinan. "Aircraft conceptual design optimization with uncertain

- contributing analyses." In *AIAA Modeling and Simulation Technologies Conference*, p. 6237. 2009.
- [9] Maughmer, Mark D. "Design of winglets for high-performance sailplanes." *Journal of Aircraft* 40, no. 6 (2003): 1099-1106.
- [10] Boermans, L. M. M., F. Nicolosi, and K. Kubrynski. "Aerodynamic design of high-performance sailplane wing-fuselage combinations." In *XXI ICAS Congress, Melbourne, Australia*, vol. 18. 1998.
- [11] Yahaya, N., A. M. M. Ismail, N. A. Sabrin, Nurrul Amilin, A. Nalisa, Ilya Izyan, and Y. Ramli. "Investigation of Whitcomb's Winglet Flow Behaviour using PIV and FLUENT." *Journal of Advanced Research in Fluid Mechanics and Thermal Sciences* 13 (2015): 22-28.
- [12] A. Munshi, E. Sulaeman, N. Omar, and M. Y. Ali, "CFD Analysis on the Effect of Winglet Cant Angle on Aerodynamics of ONERA M6 Wing," *Journal Advance Research Fluid Mechanic Thermal Science* 1, no. 1, (2018): 44–54.
- [13] Rudnick, Daniel L., Russ E. Davis, Charles C. Eriksen, David M. Fratantoni, and Mary Jane Perry. "Underwater gliders for ocean research." *Marine Technology Society Journal* 38, no. 2 (2004): 73-84.
- [14] Sun, Chunya, Baowei Song, Peng Wang, and Xinjing Wang. "Shape optimization of blended-wing-body underwater glider by using gliding range as the optimization target." *International Journal of Naval Architecture and Ocean Engineering* 9, no. 6 (2017): 693-704.
- [15] Xie, Lingwang, Xingwei Zhang, Pan Luo, and Panpan Huang. "Numerical study on the aerodynamic characteristics of both static and flapping wing with attachments." In *Journal of Physics: Conference Series*, vol. 916, no. 1, p. 012007. IOP Publishing, 2017.
- [16] S. P. Uppu, D. Manisha, G. D. Devi, and P. Chengalwa, "Aerodynamic Analysis of a Dragonfly," *Journal Advance Research Fluid Mechanic Thermal Science J.*, 1, no. 1, (2018): 31–41.
- [17] Ali, Jaffar Syed Mohamed, and M. Mubin Saleh. "Experimental and Numerical Study on the Aerodynamics and Stability Characteristics of a Canard Aircraft."
- [18] M. Selig, J. J. Guglielmo, A. P. Broeren, and P. Giguere, *Summary of Low-Speed Airfoil Data*, vol. 2. Illinois: SoarTech Publications, 1995.
- [19] Michael. "Low Reynolds number airfoil design lecture notes." *VKI lecture series* (2003): 24-28.
- [20] Javaid, Muhammad Yasar, Mark Ovinis, Fakhruddin BM Hashim, Adi Maimun, Yasser M. Ahmed, and Barkat Ullah. "Effect of wing form on the hydrodynamic characteristics and dynamic stability of an underwater glider." *International Journal of Naval Architecture and Ocean Engineering* 9, no. 4 (2017): 382-389.
- [21] S. Frati, *L'ALIANTE, The Glider*. 1946.